

## Research



**Cite this article:** Chavoshi SZ, Xu S, Goel S. 2017 Addressing the discrepancy of finding the equilibrium melting point of silicon using molecular dynamics simulations. *Proc. R. Soc. A* **473**: 20170084. <http://dx.doi.org/10.1098/rspa.2017.0084>

Received: 4 February 2017

Accepted: 5 May 2017

### Subject Areas:

materials science, nanotechnology, statistical physics

### Keywords:

melting point, silicon, molecular dynamics, Tersoff-ARK, Tersoff potential

### Author for correspondence:

Saeed Zare Chavoshi  
e-mail: [s.zare@imperial.ac.uk](mailto:s.zare@imperial.ac.uk)

# Addressing the discrepancy of finding the equilibrium melting point of silicon using molecular dynamics simulations

Saeed Zare Chavoshi<sup>1</sup>, Shuozhi Xu<sup>2</sup> and Saurav Goel<sup>3</sup>

<sup>1</sup>Department of Mechanical Engineering, Imperial College London, London SW7 2AZ, UK

<sup>2</sup>GWW School of Mechanical Engineering, Georgia Institute of Technology, Atlanta, GA 30332-0405, USA

<sup>3</sup>School of Aerospace, Transport and Manufacturing, Cranfield University, Cranfield MK43 0AL, UK

SZC, 0000-0002-2364-455X

We performed molecular dynamics simulations to study the equilibrium melting point of silicon using (i) the solid–liquid coexistence method and (ii) the Gibbs free energy technique, and compared our novel results with the previously published results obtained from the Monte Carlo (MC) void-nucleated melting method based on the Tersoff-ARK interatomic potential (Agrawal *et al. Phys. Rev. B* **72**, 125206. (doi:10.1103/PhysRevB.72.125206)). Considerable discrepancy was observed (approx. 20%) between the former two methods and the MC void-nucleated melting result, leading us to question the applicability of the empirical MC void-nucleated melting method to study a wide range of atomic and molecular systems. A wider impact of the study is that it highlights the bottleneck of the Tersoff-ARK potential in correctly estimating the melting point of silicon.

## 1. Introduction

Near-melting phenomena are rather complex and detailed explanations of the thermodynamic mechanisms involved in the melting process are somewhat unclear in the literature and so are the methods employed to estimate the melting temperature [1]. In the past, various numerical techniques including the molecular dynamics (MD) method have been employed to estimate the equilibrium melting point of various materials.

According to Zhang & Maginn [2], the methods for the calculation of the melting point can be categorized into the following:

- (i) Direct methods, including one-phase [3,4], hysteresis [5], void-nucleated [6–12] and solid–liquid coexistence [13–17] methods.
- (ii) Gibbs free energy-based methods (thermodynamic integration method [18–24]), such as Hoover and Ree’s single-occupancy cell [25,26], Frenkel and Ladd’s Einstein crystal [27] and the pseudo-supercritical path [28].

Among the direct methods, the solid–liquid coexistence method is a reliable choice in which the melting point could be bracketed within a desired interval; however, it requires a relatively large simulation cell and multiple simulation runs, and is thus a time-consuming method. In the free energy method, the Gibbs free energy of the solid and liquid phases is computed at different temperatures, and then the melting point is assumed to be the temperature at which both phases exhibit the same Gibbs free energies. Calculation of the melting temperature through introduction of voids in a perfect crystal to avoid overestimation of the melting point is another approach known as the void-nucleated method. As per this method, an increase in the size of the void causes the melting temperature versus void size curve to first exhibit a decrease and then to attain a plateau region where the melting point becomes independent of the size of the voids. The temperature of this plateau region is taken, empirically, as the thermodynamic melting point of the material. Agrawal *et al.* [6–8] in their exploratory works noted that the theoretical basis and in-depth thermodynamic considerations for this method are not established, making this method empirical in nature. In this work, we present an MD simulation case study by comparing the simulated equilibrium melting point of silicon using (i) the solid–liquid coexistence method, (ii) the Gibbs free energy method, and (iii) published results obtained using the void-nucleated method. Our simulations were informed by the Tersoff-ARK potential [6], which was categorically developed with the motivation to accurately describe the melting point and the density of the liquid phase of silicon.

## 2. Computational details and results

We employed an open-source code LAMMPS [29] to study the solid–liquid coexistence method to obtain the phase instability temperature ( $T_{\text{ins}}$ ) of silicon crystal using the one-phase method. A  $15 \times 15 \times 15$  supercell of silicon containing 27 000 atoms was heated in the canonical ensemble (NVT). To avoid the so-called hysteresis phenomenon, a low heating rate of  $9 \times 10^9 \text{ K s}^{-1}$  was used to permit the solid atoms to gently attain thermodynamic equilibrium. Also, reflective boundaries were used to avoid the spurious effects of superheating of the cell while using periodic boundary conditions (PBCs). As shown in figure 1,  $T_{\text{ins}}$  was obtained as 1397 K. At this critical value of  $T_{\text{ins}}$ , the value of the Lindemann index [30] experiences an upward jump due to a destabilized cluster of atoms caused by thermal excitation [31]. This critical value of temperature is referred to as the first-order melting transition. It is believed that the solid–liquid transition starts with nucleation in order to overcome the Gibbs free energy barrier to the formation of a nucleus of the daughter phase (namely, via thermal fluctuation) [5]. The bulk molten temperature ( $T_{\text{em}}$ ) was found to be 1616 K. The structural changes during melting (from covalent to metallic) cause an atomic volume shrinkage (calculated using Voronoi tessellation [32]) of approximately 9.2%, which is consistent with the reported experimental values [33,34]. Apart from the solid–liquid coexistence method, the hysteresis method [5] with PBCs was also employed; however, the supercooling temperature ( $T^-$ ) was not realized. In general, apart from some special cases,  $T^-$  is immensely difficult to obtain as crystal nucleation is a rare event [2].

The phase instability temperature obtained by the one-phase method can be used as an initial estimate for the solid–liquid coexistence simulation to bracket the melting point. For this purpose, a simulation box comprising  $m \times n \times l$  periodic solid cells was employed in a way that the longer direction  $\langle 001 \rangle$  lies normal to the solid–liquid interface. The system was then equilibrated near

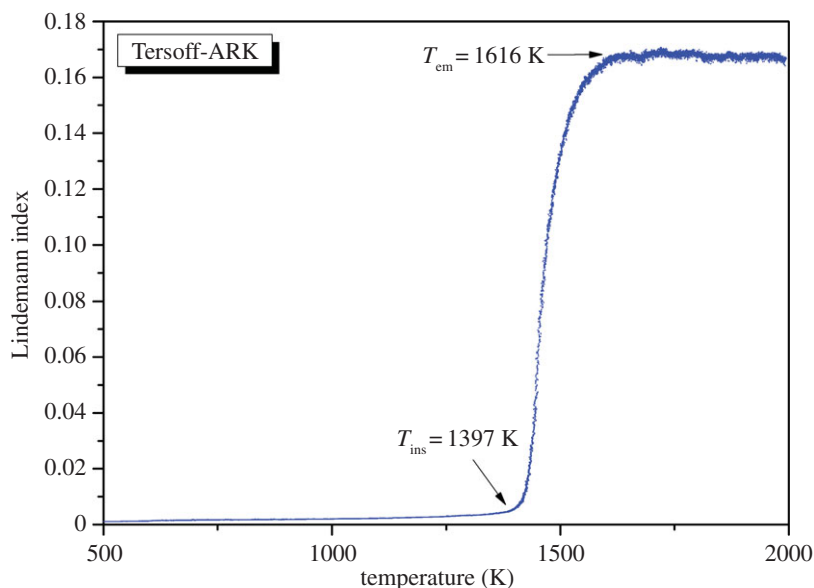


**Figure 1.** Variation of the Lindemann index upon gradual heating.  $T_{\text{ins}}$  corresponds to the phase instability temperature (or first-order melting transition temperature), while  $T_{\text{em}}$  corresponds to the bulk molten temperature of silicon. (Online version in colour.)

the initial guess of melting temperature in the isobaric–isothermal ensemble (NPT). To preserve the hydrostatic pressure conditions, an anisotropic barostat was employed. To prepare the solid–liquid coexisting system, the central half of the system was heated and melted at a fairly high temperature under the NVT ensemble, whereas the other half of the cell was kept fixed. The melted half of the system was then further equilibrated in the NPT ensemble at the initially estimated melting temperature and zero pressure. During equilibration of the melted half, the other half was kept fixed and the length of the system in the (001) direction was permitted to relax. Then, the solid and liquid halves were brought into contact and the system was equilibrated in the NPT ensemble at the same temperature to zero the (001) direction pressure. To abate the impact of non-hydrostatic stresses on the melting temperature, the simulation cell was further relaxed in the NPT ensemble with the anisotropic barostat. The entire simulation was repeated at different temperatures until the melting temperature converged. One may question whether the melting temperature is size dependent owing to the increased fraction of loosely bounded surface atoms at reduced dimension [35]. To answer this question, a convergence check was performed to determine the dependence of the estimated melting point on the size of the simulation box. Figure 2 compares the evolution of the average potential energy per atom of the solid–liquid coexistence for two different system sizes at different temperatures simulated for a relatively longer simulation time (10 ns). Figure 2*a* shows that, for a 320-atom simulation cell, when the temperature is below 1410 K, the average potential energy of the solid–liquid coexistence system decreases with time, indicating that the crystal phase tends to grow and the system solidifies. Contrary to this, at temperatures above 1415 K, the potential energy increases, suggesting that the simulation cell undergoes melting transition. Accordingly, the equilibrium melting temperature of silicon for a 320-atom simulation cell was obtained as  $1412.5 \pm 2.5$  K. Likewise, as depicted in figure 2*b*, the equilibrium melting temperature of silicon for a 108 000-atom simulation box was determined as  $1365 \pm 5$  K. Figure 3*a* presents the calculated melting point versus the number of atoms in MD simulations, where the calculated melting point converges for a simulation cell containing approximately 20 800 atoms. We infer that the calculation of the melting point using simulation cells containing fewer than 320 atoms was non-trivial owing to the high levels of energy fluctuations. In all, according to figure 3*a*, the equilibrium melting temperature of silicon

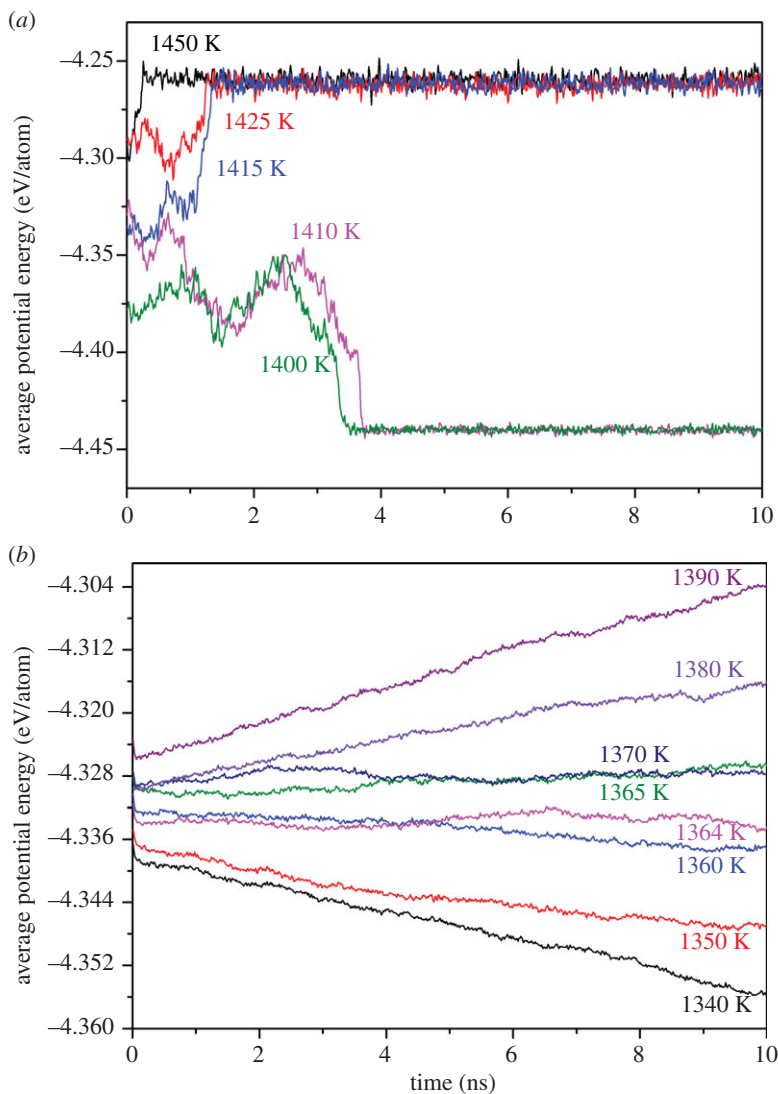


**Figure 2.** Evolution of the average potential energy of the solid–liquid coexistence cell versus the simulation time at various temperatures for (a) a 320-atom simulation cell and (b) a 108 000-atom simulation cell. (Online version in colour.)

using the solid–liquid coexistence method is  $1365 \pm 5$  K. Notice that there are implications that the melting point is slightly crystallographic orientation dependent; however, the variation is much less than the variation of the melting point caused by changing the number of atoms in the simulation box.

We also employed the Gibbs free energy technique to calculate the melting point of silicon with the same potential function but using a different MD simulation toolbox, ‘MD++’ [36]. Simulation cells with different numbers of atoms were constructed using PBCs along all three directions. At zero pressure, the Helmholtz free energy of the solid phase  $F_S$  at 1300 K was calculated by adiabatic switching from the solid phase described by the actual potential model to the harmonic approximation of the same potential function [37]. As the equilibrium volume was achieved during this process,  $F_S$  can be inferred as the Gibbs free energy at zero pressure. Then, the Gibbs free energy for the solid phase  $G_S$  as a function of temperature in the range of  $1300 \text{ K} < T < 1500 \text{ K}$  (in increments of 0.02 K) was calculated using the reversible scaling method [38]. For the liquid phase, the Helmholtz free energy (also the Gibbs free energy) at zero pressure and 1500 K was calculated by adiabatic switching from the liquid to a purely repulsive potential

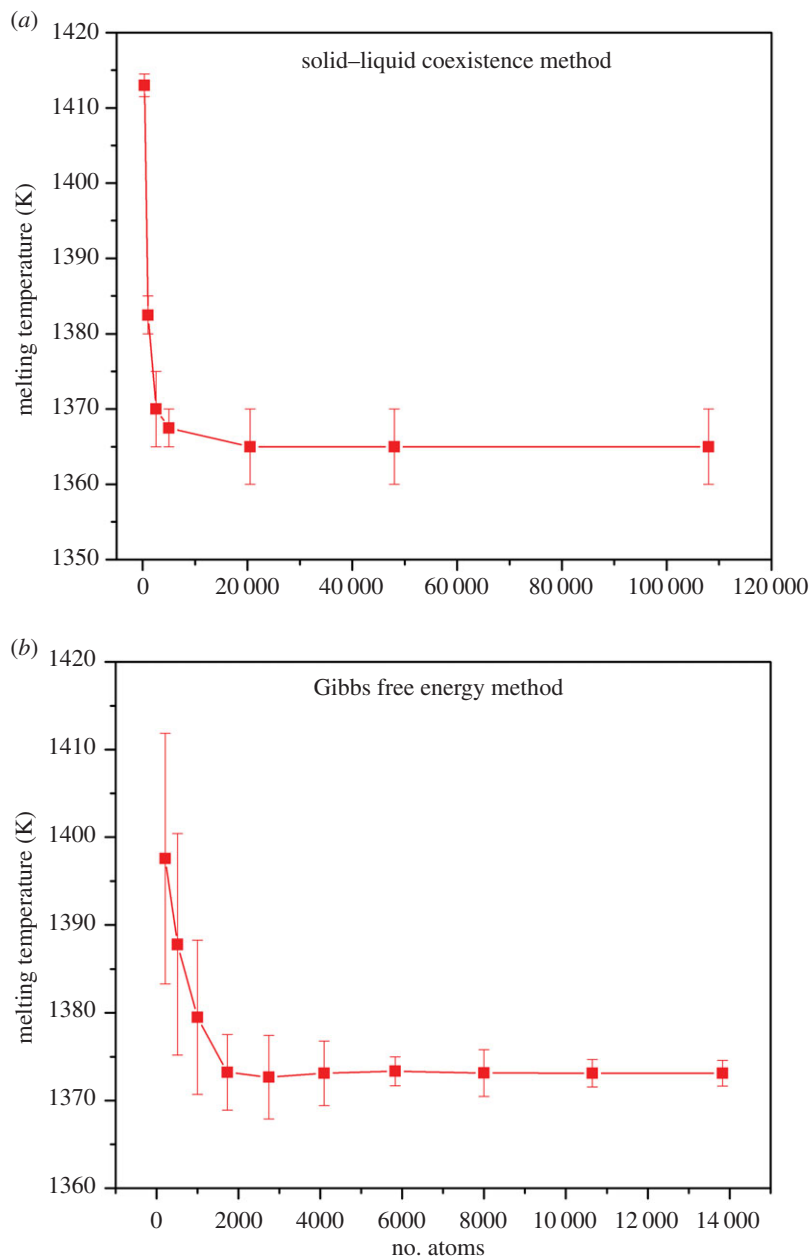


**Figure 3.** The calculated melting point versus the number of atoms in the MD simulation cell using (a) the solid-liquid coexistence method and (b) the Gibbs free energy method. (Online version in colour.)

and then to the ideal gas limit. Again, the Gibbs free energy for the liquid phase  $G_L$  as a function of temperature between 1200 K and 1500 K was calculated using the reversible scaling method [38]. In the end, both  $G_S$  and  $G_L$  were plotted as a function of temperature  $T$  on the same scale and the melting temperature was determined as the intersection of the two curves [39,40]. Figure 4 shows the Gibbs free energy per atom of both the solid phase and the liquid phase for two different supercells. The results of the convergence study are shown in figure 3b, where the equilibrium melting point is determined as  $1373 \pm 1.5$  K. Overall, figure 3 also suggests that the Gibbs free energy method converges for a smaller number of atoms (approx. 2000 silicon atoms) as opposed to the solid-liquid coexistence method, which requires about 20 000 silicon atoms to converge.

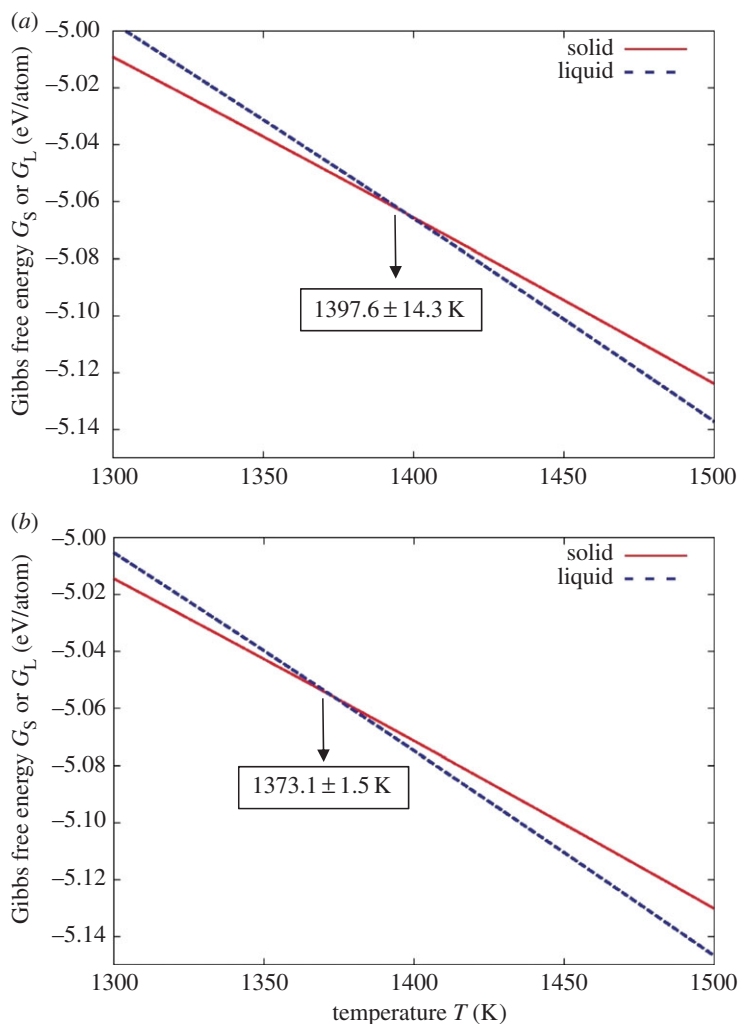


**Figure 4.** Gibbs free energy per atom for both the solid phase and the liquid phase for (a) a 216-atom simulation cell and (b) a 13 824-atom simulation cell. (Online version in colour.)

We did not perform the void-nucleated calculations and have taken these data directly from the developers of the Tersoff-ARK potential. Agrawal *et al.* [6] deployed the Monte Carlo (MC) simulations of the void-nucleated melting method and reported the melting point of silicon as 1711 K, which is approximately 20% higher than we obtained from the solid–liquid coexistence method ( $1365 \pm 5$  K) and the Gibbs free energy method ( $1373.1 \pm 1.5$  K) using the same Tersoff-ARK potential. It is imperative to note that the simulation size used by the developers of the Tersoff-ARK potential is very small (216 silicon atoms), and it is not clear how the size effect has influenced the calculated melting temperature in the presence of voids. Of interest is that the MC void-nucleated melting method was used to estimate the melting point of silicon given by the original Tersoff potential [41,42], and the value obtained was around 2509 K [6], which is in fair accordance with the results of the solid–liquid coexistence method (2584 K [43]); therefore the system size (216 atoms) seems to be a less influential factor in the reported erroneous value of the melting point of silicon obtained by the developers of the Tersoff-ARK potential. The authors posit that either the introduction of voids in such a small simulation box or the improper postulation of considering the transition temperature in the plateau region as the melting point may have led to incorrect estimations of the melting point in the Tersoff-ARK paper.

On the other hand, the work of the Koning *et al.* [44] suggests that the source of such a discrepancy can be the hysteresis occurring in the void-nucleated method. They reported that the melting point of argon given by the MD void-nucleated method [11] is 5% higher than that of the thermodynamic results. In another study carried out by Agrawal *et al.* [8], the MD void-nucleated melting method overestimated the melting point of nitromethane by up to 4% as opposed to the solid–liquid coexistence method. Zhang & Maginn [2] conducted an interesting study showing that at least three ‘plateau’ temperatures (approx. 500 K, approx. 450 K and approx. 350 K) were recognizable for a complex atomistic model of the ionic liquid 1-*n*-butyl-3-methylimidazolium chloride [BMIM][Cl] while using the MD void-nucleated method, posing a key question as to which plateau temperature corresponds to the true melting temperature. We emphasize that the results obtained in our work are based on two rigorous and accurate techniques and the fact that the experimental value of the melting point of silicon is about 1687 K [45].

### 3. Concluding remarks

In this work, we have calculated and compared the equilibrium melting point of silicon using three techniques, namely the MD solid–liquid coexistence, the MD Gibbs free energy and the MC void-nucleation techniques. The former two methods provide a close approximation while the latter method revealed a 20% discrepancy with respect to the former two methods. Our results cast doubt on the validity of the empirical assumption used in the MC void-nucleated method that the melting temperature in the plateau region near the critical void size is the true melting point. These results identify the bottleneck of the Tersoff-ARK potential in correctly estimating the melting point of silicon.

**Data accessibility.** This article has no supporting data.

**Authors' contributions.** S.Z.C. developed the idea presented here, designed the study and drafted the manuscript. S.Z.C. and S.X. carried out the computational work and participated in the data analysis. S.G. reviewed the article. All authors gave their final approval for publication.

**Competing interests.** We declare we have no competing interests.

**Funding.** S.Z.C. gratefully acknowledges the financial support from the AVIC Centre for Materials Characterisation, Processing and Modelling at Imperial College London. S.X. acknowledges the use of the Extreme Science and Engineering Discovery Environment (XSEDE), which is supported by National Science Foundation grant no. ACI-1053575. S.G. acknowledges various forms of support obtained from the European COST Action CA15102 of the Horizon 2020 programme as well as financial support from the ‘Short Term Scientific Mission’ from the COST Action MP1303 which helped with some of the ideas presented in this work.

**Acknowledgements.** The authors thank Prof. Wei Cai, Dr Yanming Wang and Dr Xiaohan Zhang from Stanford University for their advice regarding using the MD++ code.

### References

1. Bai X-M, Li M. 2006 Nucleation and melting from nanovoids. *Nano Lett.* **6**, 2284–2289. (doi:10.1021/nl0617282)
2. Zhang Y, Maginn EJ. 2012 A comparison of methods for melting point calculation using molecular dynamics simulations. *J. Chem. Phys.* **136**, 144116. (doi:10.1063/1.3702587)
3. Holender JM. 1990 Molecular-dynamics studies of the thermal properties of the solid and liquid fcc metals Ag, Au, Cu, and Ni using many-body interactions. *Phys. Rev. B* **41**, 8054–8061. (doi:10.1103/PhysRevB.41.8054)
4. Raty J-Y, Schwegler E, Bonev SA. 2007 Electronic and structural transitions in dense liquid sodium. *Nature* **449**, 448–451. (doi:10.1038/nature06123)
5. Luo S-N, Strachan A, Swift DC. 2004 Nonequilibrium melting and crystallization of a model Lennard-Jones system. *J. Chem. Phys.* **120**, 11 640–11 649. (doi:10.1063/1.1755655)
6. Agrawal PM, Raff LM, Komanduri R. 2005 Monte Carlo simulations of void-nucleated melting of silicon via modification in the Tersoff potential parameters. *Phys. Rev. B* **72**, 125206. (doi:10.1103/PhysRevB.72.125206)

7. Agrawal PM, Rice BM, Thompson DL. 2003 Molecular dynamics study of the effects of voids and pressure in defect-nucleated melting simulations. *J. Chem. Phys.* **118**, 9680–9688. (doi:10.1063/1.1570815)
8. Agrawal PM, Rice BM, Thompson DL. 2003 Molecular dynamics study of the melting of nitromethane. *J. Chem. Phys.* **119**, 9617–9627. (doi:10.1063/1.1612915)
9. Lutsko J *et al.* 1989 Molecular-dynamics study of lattice-defect-nucleated melting in metals using an embedded-atom-method potential. *Phys. Rev. B* **40**, 2841–2855. (doi:10.1103/PhysRevB.40.2841)
10. Phillpot S, Lutsko JF, Wolf D, Yip S. 1989 Molecular-dynamics study of lattice-defect-nucleated melting in silicon. *Phys. Rev. B* **40**, 2831. (doi:10.1103/PhysRevB.40.2831)
11. Solca J, Dyson AJ, Steinebrunner G, Kirchner B, Huber H. 1997 Melting curve for argon calculated from pure theory. *Chem. Phys.* **224**, 253–261. (doi:10.1016/S0301-0104(97)00317-0)
12. Solca J, Dyson AJ, Steinebrunner G, Kirchner B, Huber H. 1998 Melting curves for neon calculated from pure theory. *J. Chem. Phys.* **108**, 4107–4111. (doi:10.1063/1.475808)
13. Alfè D. 2005 Melting curve of MgO from first-principles simulations. *Phys. Rev. Lett.* **94**, 235701. (doi:10.1103/PhysRevLett.94.235701)
14. Mei J, Davenport J. 1992 Free-energy calculations and the melting point of Al. *Phys. Rev. B* **46**, 21–25. (doi:10.1103/PhysRevB.46.21)
15. Morris JR, Song X. 2002 The melting lines of model systems calculated from coexistence simulations. *J. Chem. Phys.* **116**, 9352–9358. (doi:10.1063/1.1474581)
16. Morris JR, Wang CZ, Ho KM, Chan CT. 1994 Melting line of aluminum from simulations of coexisting phases. *Phys. Rev. B* **49**, 3109–3115. (doi:10.1103/PhysRevB.49.3109)
17. Ogitsu T, Schwegler E, Gygi F, Galli G. 2003 Melting of lithium hydride under pressure. *Phys. Rev. Lett.* **91**, 175502. (doi:10.1103/PhysRevLett.91.175502)
18. Fickett W, Wood W. 1960 Shock Hugoniot for liquid argon. *Phys. Fluids* **3**, 204–209. (doi:10.1063/1.1706018)
19. Levesque D, Verlet L. 1969 Perturbation theory and equation of state for fluids. *Phys. Rev.* **182**, 307–316. (doi:10.1103/PhysRev.182.307)
20. McDonald I, Singer K. 1967 Machine calculation of thermodynamic properties of a simple fluid at supercritical temperatures. *J. Chem. Phys.* **47**, 4766–4772. (doi:10.1063/1.1701695)
21. Verlet L. 1967 Computer ‘experiments’ on classical fluids. I. Thermodynamical properties of Lennard-Jones molecules. *Phys. Rev.* **159**, 98–103. (doi:10.1103/PhysRev.159.98)
22. Wood W. 1968 Monte Carlo studies of simple liquid models. In *Physics of simple liquids* (eds ANW Temperly, JS Rowlinson, GS Rushbrooke). Amsterdam: North-Holland.
23. Wood W, Parker F. 1957 Monte Carlo equation of state of molecules interacting with the Lennard-Jones potential. I. A supercritical isotherm at about twice the critical temperature. *J. Chem. Phys.* **27**, 720–733. (doi:10.1063/1.1743822)
24. Sugino O, Car R. 1995 Ab initio molecular dynamics study of first-order phase transitions: melting of silicon. *Phys. Rev. Lett.* **74**, 1823–1826. (doi:10.1103/PhysRevLett.74.1823)
25. Hoover WG, Ree FH. 1967 Use of computer experiments to locate the melting transition and calculate the entropy in the solid phase. *J. Chem. Phys.* **47**, 4873–4878. (doi:10.1063/1.1701730)
26. Hoover WG, Ree FH. 1968 Melting transition and communal entropy for hard spheres. *J. Chem. Phys.* **49**, 3609–3617. (doi:10.1063/1.1670641)
27. Frenkel D, Ladd AJ. 1984 New Monte Carlo method to compute the free energy of arbitrary solids. Application to the fcc and hcp phases of hard spheres. *J. Chem. Phys.* **81**, 3188–3193. (doi:10.1063/1.448024)
28. Eike DM, Brennecke JF, Maginn EJ. 2005 Toward a robust and general molecular simulation method for computing solid-liquid coexistence. *J. Chem. Phys.* **122**, 014115. (doi:10.1063/1.1823371)
29. Plimpton S. 1995 Fast parallel algorithms for short-range molecular dynamics. *J. Comput. Phys.* **117**, 1–19. (doi:10.1006/jcph.1995.1039)
30. Stillinger FH, Weber TA. 1980 Lindemann melting criterion and the Gaussian core model. *Phys. Rev. B* **22**, 3790–3794. (doi:10.1103/PhysRevB.22.3790)
31. Jin ZH, Gumbsch P, Lu K, Ma E. 2001 Melting mechanisms at the limit of superheating. *Phys. Rev. Lett.* **87**, 055703. (doi:10.1103/PhysRevLett.87.055703)
32. Rycroft C. 2009 *Voro++: A three-dimensional Voronoi cell Library in C++*. Lawrence Berkeley National Laboratory. See <http://math.lbl.gov/voro++/>.
33. Glazov V, Shchelikov OD. 2000 Volume changes during melting and heating of silicon and germanium melts. *High Temp.* **38**, 405–412. (doi:10.1007/BF02756000)

34. Logan R, Bond W. 1959 Density change in silicon upon melting. *J. Appl. Phys.* **30**, 322–322. (doi:10.1063/1.1735159)
35. Alavi S, Thompson DL. 2006 Molecular dynamics simulations of the melting of aluminum nanoparticles. *J. Phys. Chem. A* **110**, 1518–1523. (doi:10.1021/jp053318s)
36. Cai W. MD++ source codes and automatic scripts for free energy and melting point calculations. See <http://micro.stanford.edu/MDpp/>.
37. Watanabe M, Reinhardt WP. 1990 Direct dynamical calculation of entropy and free energy by adiabatic switching. *Phys. Rev. Lett.* **65**, 3301–3304. (doi:10.1103/PhysRevLett.65.3301)
38. Kaczmariski M, Rurali R, Hernández E. 2004 Reversible scaling simulations of the melting transition in silicon. *Phys. Rev. B* **69**, 214105. (doi:10.1103/PhysRevB.69.214105)
39. Ryu S, Cai W. 2008 Comparison of thermal properties predicted by interatomic potential models. *Model. Simul. Mater. Sci. Eng.* **16**, 085005. (doi:10.1088/0965-0393/16/8/085005)
40. Wang Y, Santana A, Cai W. 2016 Au–Ge MEAM potential fitted to the binary phase diagram. *Model. Simul. Mater. Sci. Eng.* **25**, 025004. (doi:10.1088/1361-651X/aa5260)
41. Tersoff J. 1989 Modeling solid-state chemistry: interatomic potentials for multicomponent systems. *Phys. Rev. B* **39**, 5566–5568. (doi:10.1103/PhysRevB.39.5566)
42. Tersoff J. 1990 Erratum: Modeling solid-state chemistry: interatomic potentials for multicomponent systems. *Phys. Rev. B* **41**, 3248. (doi:10.1103/PhysRevB.41.3248.2)
43. Yoo S, Zeng XC, Morris JR. 2004 The melting lines of model silicon calculated from coexisting solid–liquid phases. *J. Chem. Phys.* **120**, 1654–1656. (doi:10.1063/1.1633754)
44. de Koning M, Antonelli A, Yip S. 2001 Single-simulation determination of phase boundaries: a dynamic Clausius–Clapeyron integration method. *J. Chem. Phys.* **115**, 11 025–11 035. (doi:10.1063/1.1420486)
45. Lide D. 2003 *DR 2003–2004 CRC handbook of chemistry and physics*. Boca Raton, FL: CRC Press.